An active energy management distributed formation control for tethered space net robot via cooperative game theory

Yifeng Ma, Yizhai Zhang, Ya Liu, Panfeng Huang, Fan Zhang

PII: S0094-5765(24)00651-9

DOI: https://doi.org/10.1016/j.actaastro.2024.11.004

Reference: AA 10788

To appear in: Acta Astronautica

Received date: 30 July 2024

Revised date: 26 September 2024 Accepted date: 2 November 2024



Please cite this article as: Y. Ma, Y. Zhang, Y. Liu et al., An active energy management distributed formation control for tethered space net robot via cooperative game theory, *Acta Astronautica* (2024), doi: https://doi.org/10.1016/j.actaastro.2024.11.004.

This is a PDF file of an article that has undergone enhancements after acceptance, such as the addition of a cover page and metadata, and formatting for readability, but it is not yet the definitive version of record. This version will undergo additional copyediting, typesetting and review before it is published in its final form, but we are providing this version to give early visibility of the article. Please note that, during the production process, errors may be discovered which could affect the content, and all legal disclaimers that apply to the journal pertain.

© 2024 Published by Elsevier Ltd on behalf of IAA.

An Active Energy Management Distributed Formation Control for Tethered Space Net Robot via Cooperative Game Theory

Yifeng Ma^{a,b}, Yizhai Zhang^{a,b}, Ya Liu^{a,b}, Panfeng Huang^{a,b}, Fan Zhang^{a,b,*}

^aThe Research Center for Intelligent Robotics School of Astronautics Northwestern Polytechnical University Xi'an Shaanxi 710072 China.

^bShaanxi Province Innovation Team of Intelligent Robotic Technology Xi'an Shaanxi 710072 China.

^cSchool of Electronic Information and Electrical Engineering Shanghai Jiao Tong University Shanghai 200240 China.

Abstract

The current studies for Tethered Space Net Robot (TSNR) typically treat the tension force induced by the net as a disturbance and employ passive suppression for compensation. However, these approaches not only result in excess fuel consumption but also overlook the intrinsic nature of the net dynamics. When one Maneuverable Unit (MU) maneuvers, it generates a tension force on the net that is transmitted to other MUs. This force not only affects the control accuracy of other MUs but also has a positive effect. In this paper, an Active Energy Management Distributed Formation Control (AEMC) strategy is proposed to reveal this kind of interaction and maximize its advantage. Firstly, an energy recovery framework is established, allowing each MU can effectively utilize the tension force due to the net. Specifically, a neural network estimator is designed to capture the hysteresis relationship in which MUs influence each other by transmitting forces through the net. Furthermore, to achieve the cooperative completion of tasks, a game based control scheme is proposed to optimize the control input and tension force collectively. Through prediction and optimization, MUs actively manage their impacts on each other, thereby controlling the influence of tension force on the tracking errors of others. Finally, numerical simulations are conducted to showcase the effectiveness of the proposed approach.

Keywords: Tethered Space Net Robot, Formation control, Differential cooperative games, Learning-based control

1. Introduction

On-orbit services, such as debris removal and the capture of noncooperative targets, are emerging as promising trends in future space development [1]. Over the past few decades, various flexible tethered space systems have been proposed to facilitate capture missions. These systems, such as the Tethered Space Net (TSN) [2], Tethered Space Robot (TSR) [3], Tethered Space Net Robot (TSNR) [4], and other [5], utilize a flexible tether to connect the capturing device and the target. Tethered Space Net Robot (TSNR) emerges as an innovative solution for active space debris capture and removal, as illustrated in Fig. 1. Its expansive envelope and straightforward capture method render it an appealing choice for such tasks. However, control challenges arise when attempting to capture debris with the flexible and elastic underactuated net.

Email address: fzhang@nwpu.edu.cn (Fan Zhang)

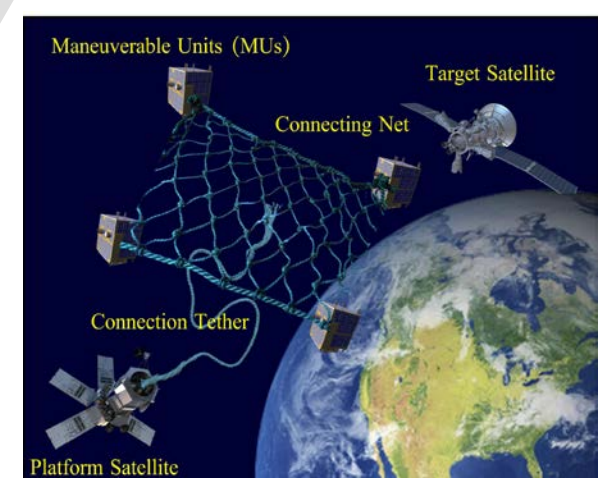


Fig. 1. TSNR system.

^{*}Corresponding author at: 127 West Youyi Road, Beilin District, Xi'an Shaanxi, 710072, China.

In recent years, researchers have extensively explored control challenges associated with TSNR for space debris capture tasks. For example, the study in [6] formulated formation-keeping control strategies, employing two artificial potential functions to preserve the TSNR's configuration while adhering to relative distance constraint. Additionally, Zhang et al. [7] introduced a fuzzy-based adaptive super-twisting sliding mode control to estimate and suppress the complex oscillations of the TSNR. Liu et al. [8] designed a capture configuration optimization method and an observer base timevarying formation tracking control algorithm, considering contact dynamics with realistic space debris.

However, prior studies have primarily focused on overarching control objectives, overlooking the importance of individual subjective initiative. Treating the extra tension force caused by other MUs as mere perturbations result in excess fuel consumption which is precisous for a spacecraft, and fails to adequately capture dynamic interactions among MUs. Game theory serves as a fitting analytical method for addressing interaction formation issues within multi-agent systems. Jiang et al. [9] introduced the cooperative error into the cost function to study the consistency of the formation. Additionally, Li et al. [10] explored a distributed game strategy for the formation control of multi-spacecraft, introducing a worst-case Nash strategy against the disturbance defined as a player. The study in [11] investigated the problem of modular robots cooperating in handling a large space structure by using the framework of cooperative game, and designed a coordinated compensatory control mechanism using the principle of model predictive control, which ensures that it is able to track the desired optimal handling trajectory. Liu et al. [12] extended the application of differential graphical game control to the coupled non-linear dynamics of the T-MRUAVs system by introducing a sophisticated framework, capturing the collaborative and competitive nature among UAVs to achieve efficient and secure stability control of the system.

Nonetheless, current game theory based methods designed for multi-agent systems are not directly applicable to TSNR. In existing work, the game model typically has a deterministic form, allowing for a visual depiction of the effect of each individual in the multi-agent system on the game state. However, MUs in TSNR interact with each other by transferring tension forces through the net, raising the question of how to describe this implicit and time-delayed relationship. In this work, a neural network based tension force estimator is proposed to estimate and predict this complex relationship among MUs. For treating the tension force as a perturbation,

both the fixed-time [13, 14] or finite-time [15, 16] state observer can effectively estimate the perturbation, while sensors or camera can be employed to measure the external force. Recently, machine-learning scheme has emerged as attractive approaches for modelling complex dynamics or external forces [17, 18, 19, 20], owing to their learning and fitting ability. However, these methods often struggle to describe this kind of hysteresis relationship between tension force and individual state.

To address the aforementioned problems, a novel cooperative game theory based formation control scheme (AEMC) for TSNR is proposed in this paper. In this scheme, the tension force of the net is no longer considered as a mere perturbation. Instead, forces acting on other MUs generated by one MU's maneuver are concretely characterized. The advantages of this interaction are further explored and exploited, enhancing formation control capabilities. The main contributions of this work are outlined as follows:

- 1. An active energy management framework is established to mitigate the negative effects and capitalize on the positive effects of tension force, which is no longer compensated for in a blanket manner and produces excess fuel consumption. Instead, tension forces are actively managed by each MU.
- 2. Tension forces are transmitted among MUs through the net like ocean waves, where these forces are not only influenced by the current state but also by the past states. To effectively depict this kind of hysteresis interaction among MUs, a Deep Neural Network (DNN) based tension force estimator is proposed in this paper to estimate and predict tension force.
- 3. After obtaining the force interactions among MUs, a distributed cooperative game theory based control scheme is designed. Unlike passive compensation formation control methods [7, 8], in this scheme, through information exchange and gaming, one MU can actively manage the impact of tension force on the tracking errors of other MUs, thus being able to cooperate better in the capture task.

The remainders are stated as follows. Section 2 presents the mission and dynamic model of TSNR. In Section 3, a novel active energy management formation control strategy is proposed. In Section 4, the proposed scheme is validated using numerical simulations and results. Section 5 concludes this paper.

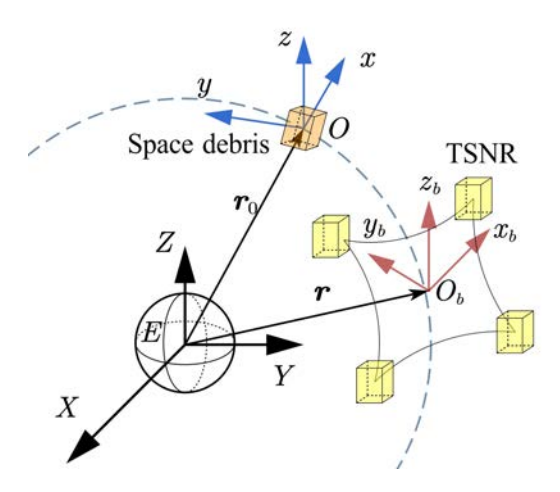


Fig. 2. Coordinate frames of TSNR system.

2. Problem formuation

2.1. Mission description

This paper focuses on the application of TSNR to complete an on-orbit debris removal service to capture space debris or failed satellites. First, the net is folded and four MUs are clustered together. When a target is detected, the four MUs carrying the net are ejected from the platform satellite. Then four MUs manoeuvre to unfold the net and approach the target, maintaining an easy-capture configuration. Finally, four MUs drive the net to envelope the target and complete the capture mission.

2.2. Dynamic model of TSNR

To describe the movements of TSNR and space debris, the following coordinate frames are first introduced (as depicted in Fig. 2). The Earth-Centered Inertial (ECI) frame, denoted by EXYZ, is located at the center of the Earth. The non-inertial Local Vertical Local Horizontal (LVLH) orbit coordinate frame, denoted by Oxyz, is located at the target. TSNR only undergoes translation relative to the target, and the relative distance is much smaller than the orbital radius. Furthermore, the body-fixed frame denoted by Obxbybzb and located at the center of TSNR, is parallel to the orbital coordinate frame.

The relative dynamics equation between space debris and TSNR in inertial frame can be expressed by the following equation:

$$\begin{cases} \ddot{\mathbf{r}}_0 = -\frac{\mu r_0}{r_0^3} \\ \ddot{\mathbf{r}}_{ij} = -\frac{\mu r_{ij}}{r_{ij}^3} + \mathbf{u}_{ij} + \mathbf{T}_{ij} \end{cases}$$
(1)

where \mathbf{r}_0 and \mathbf{r}_{ij} denote the position of space debris and any net node of TSNR respectively, with $\mathbf{r}_0 = ||\mathbf{r}_0||$ and $\mathbf{r}_{ij} = ||\mathbf{r}_{ij}||$; μ is the gravitation constant; \mathbf{u}_{ij} and \mathbf{T}_{ij} represent control input and tension force on node ij. The dynamic model of node ij which expresses the relative motion in LVLH frame can be written as:

$$\begin{cases} \ddot{x}_{ij} - 2\omega \dot{y}_{ij} - \omega^2 x_{ij} - \dot{\omega} y_{ij} = \frac{2\mu x_{ij}}{r_0^3} + u_{ij}^x + T_{ij}^x \\ \ddot{y}_{ij} + 2\omega \dot{x}_{ij} - \omega^2 y_{ij} + \dot{\omega} x_{ij} = -\frac{\mu y_{ij}}{r_0^3} + u_{ij}^y + T_{ij}^y \\ \ddot{z}_{ij} = -\frac{\mu z_{ij}}{r_0^3} + u_{ij}^z + T_{ij}^z \end{cases}$$
(2)

where ω is the orbital frequency of the debris; $\boldsymbol{u}_{ij} = \begin{bmatrix} u_{ij}^x, u_{ij}^y, u_{ij}^z \end{bmatrix}^{\mathrm{T}}$ and $\boldsymbol{T}_{ij} = \begin{bmatrix} T_{ij}^x, T_{ij}^y, T_{ij}^z \end{bmatrix}^{\mathrm{T}}$. Define the node ij's state as $\boldsymbol{x}_{ij} = \begin{bmatrix} x_{ij}, y_{ij}, z_{ij}, \dot{x}_{ij}, \dot{y}_{ij}, \dot{z}_{ij} \end{bmatrix}^{\mathrm{T}}$, and model (2) can be rearranged as:

$$\dot{\boldsymbol{x}}_{ij} = \boldsymbol{A}(r_0, \omega, \dot{\omega})\boldsymbol{x}_{ij} + \boldsymbol{B}(\boldsymbol{u}_{ij} + \boldsymbol{T}_{ij}) \tag{3}$$

What makes dynamics of TSNR most different from other space robots is the tension force T_{ij} generated by the flexible net. Inside the net, each mesh edge between two adjacent nodes is simplified as spring-damping model. Therefore, the tension force of node ij is calculated as:

$$T_{ij} = \sum_{kh \in N_{ij}} T_{ij-kh}$$

$$= \begin{cases} \left(\frac{EA}{l_n} \Delta l_{ij-kh} + c\dot{l}_{ij-kh}\right) \hat{\boldsymbol{l}}_{ij-kh} & \Delta l_{ij-kh} \geqslant 0\\ 0 & \Delta l_{ij-kh} < 0 \end{cases}$$
(4)

where N_{ij} is the set of nodes connected to node ij; T_{ij-kh} is the tension force between node ij and kh; l_n and l_{ij-pq} denote the length of mesh edge and actual length of the two nodes; $\Delta l_{ij-kh} = l_{ij-kh} - l_n$ is the elongation of mesh edge; E is Young's modulus of the net material; A represents the horizontal area of mesh edge; e is damping coefficient; \hat{l}_{ij-kh} is unit vector from node ij to kh.

Remark 1. TSNR is a underactuated system, which can only be controlled indirectly by four MUs on the corner of the net. These MU nodes are noted as MU 1-4, and dynamics of MU i can be obtained as:

$$\dot{\boldsymbol{x}}_i = \boldsymbol{A}(r_0, \omega, \dot{\omega})\boldsymbol{x}_i + \boldsymbol{B}(\boldsymbol{u}_i + \boldsymbol{T}_i) \tag{5}$$

Obviously tension force can have a significant impact on MUs and configuration of the net, so the objective of control is to avoid excessive tension forces, and to maintain microtension for net stabilisation. The control method will be discussed in the next section.

2.3. Graph theory

In TSNR system, the directed graph \mathcal{G} represents the network structure facilitating information exchange among MUs. The adjacency matrix $\mathcal{A} = \begin{bmatrix} a_{ij} \end{bmatrix} \in \mathbb{R}^{n \times n}$, where $a_{ij} > 0$ if MU i can directly receive infromation from its neighbor MU j, and $a_{ij} = 0$ otherwise. The set of neighbors of MU i is defined as N_i . And the indegree matrix $\mathcal{D} = \operatorname{diag}(d_{ii})$ is fromed by $d_{ii} = \sum_{j=1}^n a_{ij}$. Then the graph Laplacian matrix is defined as $\mathcal{L} = \mathcal{D} - \mathcal{A}$. In addition, for the problem of trajectory tracking, introduce $\mathcal{B} = \operatorname{diag}(b_1, \dots, b_n) \in \mathbb{R}^{n \times n}$, where $b_i > 0$ if MU i can obtain a desired trajectory.

3. Controller design

In this section, an active energy management distributed formation tracking control strategy is designed for TSNR (as depicted in Fig. 3), including two parts: tension force neural estimator and differential cooperative game based controller. In each time step, the neural estimator estimates and predicts tension force in real time based on the states of adjacent MUs. Then MUs optimize their own objective that contains predicted tension force, by communicating and gaming with each other.

3.1. Tension force neural network estimator

According to dynamics of TSNR (4), MU i's tension force T_i is associated with the nodes near MU i, which are also affected by their neighbors. Exploring further out of nodes, it can be found that the four MUs interact with each other by transferring forces through the net. Therefore, T_i is caused by the manoeuvres of adjacent MUs, and can be expressed as:

$$T_i = f(x_i, x_{-i}, u_i, u_{-i})$$
 (6)

where x_{-i} and u_{-i} are the states and control inputs of MU *i*'s neighbors; f is a function that represents mapping from state and control to tension force.

This function f is strongly nonlinear, and although an analytical solution can be obtained by net model (4), in practice it is unrealistic to obtain the state of each node to solve it. Meanwhile, the function has a very noticeable hysteresis. The vibrations caused by one particular MU will be transmitted to other neighboring MUs through the net like waves. Thus, the present force $T_{i,k}$ is related to the past state, and the present state will produce a new sequence of tension force in the future. Therefore, the function (6) can be deduced as:

$$T_{i}(t_{k} + N_{t}\Delta t|t_{k}) = \Phi(X_{i}(t_{k} - N_{t}\Delta t|t_{k}))$$
(7)

where N_t is predict horizon of the estimator; $T_i(t_k + N_t \Delta t | t_k)$ denotes tension force sequence $\begin{bmatrix} T_{i,k}^T, T_{i,k+1}^T, \cdots, T_{i,k+N_t-1}^T \end{bmatrix}^T$; $X_i(t_k - N_t \Delta t | t_k)$ represents state sequence $\begin{bmatrix} X_{i,k-N_t+1}^T, \cdots, X_{i,k-1}^T, X_{i,k}^T \end{bmatrix}^T$; the state is defined as $X_{i,k} = \begin{bmatrix} x_{i,k}^T, x_{-i,k}^T, u_{-i,k}^T \end{bmatrix}^T$. Furthermore, due to DNN's remarkable ability of

Furthermore, due to DNN's remarkable ability of function approximation, a DNN parameterized by weights $\theta = W^1, \dots, W^{L+1}$ is raised to approximate the nolinear and time-delayed function Φ :

$$\boldsymbol{\Phi} = W^{L+1} \phi(W^L(\cdots \phi(W^1 X_i) \cdots)) \tag{8}$$

where ϕ is the ReLU activation function. To estimate and predict tension force associated with present and past state, loss function L is formulated as:

$$L(\boldsymbol{T}_{i}, \boldsymbol{\hat{T}}_{i}) = \alpha L_{e}(\boldsymbol{T}_{i}(t_{k}), \boldsymbol{\hat{T}}_{i}(t_{k})) + \beta L_{p}(\boldsymbol{T}_{i}(t_{k} + N_{t}\Delta t|t_{k}), \boldsymbol{\hat{T}}_{i}(t_{k} + N_{t}\Delta t|t_{k}))$$

$$(9)$$

where \hat{T}_i is estimate of tension force T_i ; α and β are positive hyperparameters. Loss function $L(T_i, \hat{T}_i)$ consists of two parts: estimation L_e and prediction L_p . The purpose of the first part is to estimate exact tension force at every time step, having the following form:

$$L_{e} = \begin{cases} (1 - \gamma) \left\| \boldsymbol{T}_{i}(t_{k}) - \hat{\boldsymbol{T}}_{i}(t_{k}) \right\| & \boldsymbol{T}_{i}(t_{k}) > \hat{\boldsymbol{T}}_{i}(t_{k}) \\ \gamma \left\| \boldsymbol{T}_{i}(t_{k}) - \hat{\boldsymbol{T}}_{i}(t_{k}) \right\| & \boldsymbol{T}_{i}(t_{k}) < \hat{\boldsymbol{T}}_{i}(t_{k}) \end{cases}$$
(10)

where γ is a positive constant. Because excessive tension force can lead to net breakage or even system collapse, overestimation of tension force is permissible, while underestimation is not. Therefore γ is set in (0,0.5) to penalise underestimation.

Next, the second part is aimed to predict the change in tension force over a period of time. This can be expressed as:

$$L_{p} = \sum_{n=1}^{N_{t}} \eta_{n} \left\| \boldsymbol{T}_{i} \left(t_{k} + n \Delta t \right) - \hat{\boldsymbol{T}}_{i} \left(t_{k} + n \Delta t \right) \right\| \tag{11}$$

where $\eta_n \in (0,1)$ is a decay constant. This part of loss function focuses on forecasting tension force errors over a period time in the future. Due to the temporal delay between MUs' interactions, the current state $X_i(t_k)$ exerts a lesser influence on the force at next step $T_i(t_k + \Delta t)$. Instead, it exerts a more pronounced effect on the force at a slightly later time. So the value of η_n depends on the time.

Theorem 1. A ReLU network can approximate any function f from $F_{d,n}$ with error $\epsilon \in (0,1)$. $F_{d,n}$ is the

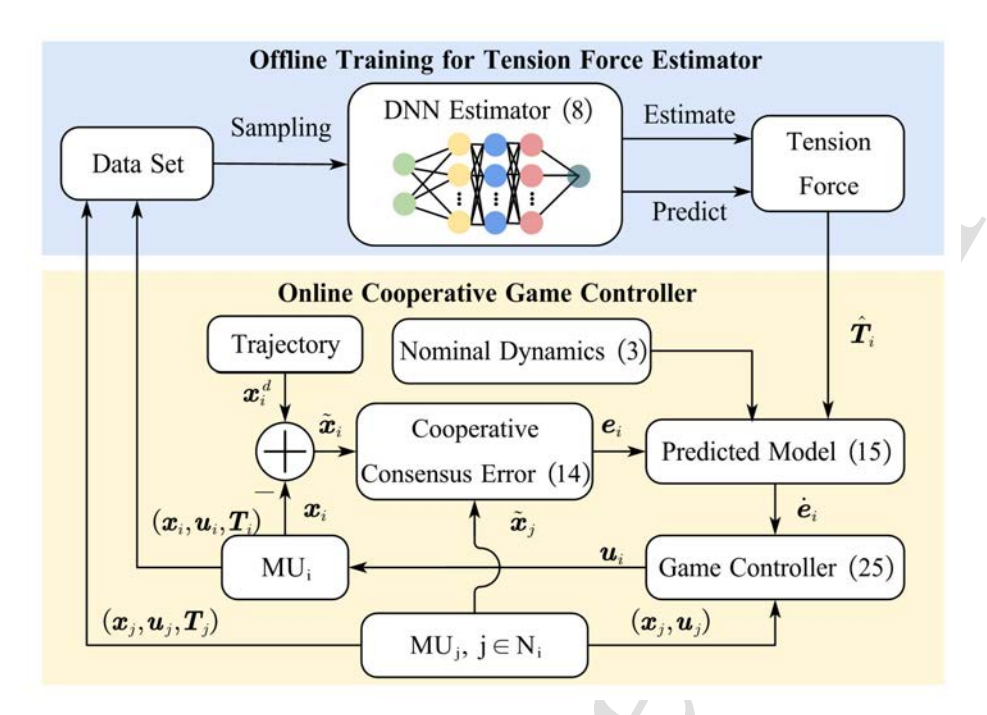


Fig. 3. System overview.

unit ball in Sobolev spaces $W^{n,\infty}([0,1]^d)$. Thus the approximation error of the designed DNN estimator (8) is bounded.

The detailed proof of Theorem 1 is derived in the appendix.

Finally, based on the predicted force \hat{T}_i obtained from the proposed estimator (8), MU i's dynamic can be rearranged as:

$$\dot{\boldsymbol{x}}_i = \boldsymbol{A}(r_0, \omega, \dot{\omega})\hat{\boldsymbol{x}}_i + \boldsymbol{B}(\boldsymbol{u}_i + \hat{\boldsymbol{T}}_i)$$
 (12)

Define $\hat{u}_i = u_i + \hat{T}_i$, predicted dynamic of MU can be reformulated as:

$$\dot{\mathbf{x}}_i = \mathbf{A}\mathbf{x}_i + \mathbf{B}\hat{\mathbf{u}}_i \tag{13}$$

Remark 2. During the data collection process, multiple trajectories of TSNR are given and the state of each moment $X_i(t_k)$ is recorded. Further the actual tension force T_i can be obtained offline by states information and (4). In order to facilitate the analysis of these data, the input and output data were normalised. This was necessary due to the large temporal span of the state, the numerous dimensions of the state, and the considerable disparity between position data and velocity ones.

3.2. Cooperative game based formation controller

The objective of each MU is not only to track its own trajectory, but also to maintain a certain formation scal-

ing, so that the net remains well configured. Define tracking error $\tilde{x}_i = x_i - x_i^d$, where x_i^d is the desired capture trajectory according to [8]. Then, the cooperative consensus error is:

$$\mathbf{e}_i = \sum_{i \in N} a_{ij} \left(\tilde{\mathbf{x}}_i - \tilde{\mathbf{x}}_j \right) + b_i \tilde{\mathbf{x}}_i \tag{14}$$

Define global error $\tilde{x} = \left[\tilde{x}_1^T, \tilde{x}_2^T, \cdots, \tilde{x}_n^T\right]^T$, the derivative of (14) has the following form:

$$\dot{\boldsymbol{e}}_{i} = ((\boldsymbol{\mathcal{L}}_{i} + \boldsymbol{\mathcal{B}}_{i}) \otimes \boldsymbol{I}) \dot{\boldsymbol{x}}
= ((l_{ii} + b_{ii}) \otimes \boldsymbol{I}) \dot{\boldsymbol{x}}_{i} + \sum_{j \in N_{i}} ((l_{ij} + b_{ij}) \otimes \boldsymbol{I}) \dot{\boldsymbol{x}}_{j}
= \boldsymbol{L}_{i} \dot{\boldsymbol{x}}_{i} + \sum_{j \in N_{i}} \boldsymbol{L}_{ij} \dot{\boldsymbol{x}}_{j}
= \boldsymbol{L}_{i} (\boldsymbol{A} \boldsymbol{x}_{i} + \boldsymbol{B} \hat{\boldsymbol{u}}_{i} - \dot{\boldsymbol{x}}_{i}^{d}) + \sum_{j \in N_{i}} \boldsymbol{L}_{ij} (\boldsymbol{A} \boldsymbol{x}_{j} + \boldsymbol{B} \hat{\boldsymbol{u}}_{j} - \dot{\boldsymbol{x}}_{j}^{d})$$
(15)

where \mathcal{L}_i is the *i* th row vector of the Laplacian matrix \mathcal{L} , i.e., $\mathcal{L}_i = [l_{i1}, \cdots, l_{in}]$. Similarly, $\mathcal{B}_i = [b_{i1}, \cdots, b_{in}]$. $\mathcal{L}_i = (l_{ii} + b_{ii}) \otimes \mathcal{I}$ and $\mathcal{L}_{ij} = (l_{ij} + b_{ij}) \otimes \mathcal{I}$. According to (15), apparently there is a cooperative relationship among MUs.

Then, by taking each MU as a game player, consensus error e_i as the game state and \hat{u}_i as the control strat-

egy, a *n*-person cooperative game is established to design the distributed formation controller for TSNR. The cost function of each player is formulated as:

$$J_{i} = \int_{t_{0}}^{t_{f}} \left(\boldsymbol{e}_{i}^{\mathsf{T}} \boldsymbol{Q}_{i} \boldsymbol{e}_{i} + \hat{\boldsymbol{u}}_{i}^{\mathsf{T}} \boldsymbol{R}_{i} \hat{\boldsymbol{u}}_{i} + \sum_{j \in N_{i}} \hat{\boldsymbol{u}}_{j}^{\mathsf{T}} \boldsymbol{R}_{ij} \hat{\boldsymbol{u}}_{j} \right) dt \qquad (16)$$

where t_0 and t_f are the initial and final time. All weighting matrices are symmetric and constant. And $Q_i > 0$, $R_i > 0$ and $R_{ij} \ge 0$. In order to suppress tracking error and realize consensus, each MU discovers the optimal control strategy by minimizing its own cost function (16). To be distributed, the control strategy \hat{u}_i of MU i only utilizes its individual state information and that of its neighbors during the gaming process.

Definition 1. (Pareto Optimal Solution)[21]. In a cooperative game composed by n players, for any two sets of control strategies $\mathbf{u}^* = \begin{bmatrix} \mathbf{u}_1^*, \cdots, \mathbf{u}_n^* \end{bmatrix}^T$ and $\mathbf{u} = \begin{bmatrix} \mathbf{u}_1, \cdots, \mathbf{u}_n \end{bmatrix}^T$, \mathbf{u}^* is said to dominate \mathbf{u} in Pareto sense if the following conditions hold:

$$\begin{cases} J_i(\boldsymbol{u}^*) \leqslant J_i(\boldsymbol{u}) & \text{for all } i \in \{1, 2, \dots n\} \\ J_i(\boldsymbol{u}^*) < J_i(\boldsymbol{u}) & \text{for at least one } i \in \{1, 2, \dots n\} \end{cases}$$
(17)

 u^* is the Pareto optimal solution if there is no other strategy dominates u^* . The Pareto optimal solution can be interpreted as a public agreement of all players, where it is impossible to improve one particular player's cost function without causing loss in any other's. It can be obtained by minimizing the following combination of all player's cost functions:

$$J = \sum_{i=1}^{n} \lambda_i J_i \tag{18}$$

where $\lambda_i \in (0, 1)$ is the weight on cost function of player i, and $\sum_{i=1}^{n} \lambda_i = 1$.

For the designed game consisting of (15) and (16), in order to obtain its Pareto optimal solution \hat{u}^* , a model predict strategy is proposed. Firstly, game model (15) must be discretised and iterated. At t_k , MU's dynamic is discretised as:

$$\boldsymbol{x}_{i,k+1} = \boldsymbol{A}_k \boldsymbol{x}_{i,k} + \boldsymbol{B}_k \hat{\boldsymbol{u}}_{i,k} \tag{19}$$

where A_k and B_k are discrete dynamic matrices. Then discretised cooperative consensu error yields the follow-

ing expression:

$$e_{i,k+1} = \mathbf{L}_{i}(\mathbf{A}_{k}\mathbf{x}_{i,k} + \mathbf{B}_{k}\hat{\mathbf{u}}_{i,k} - \mathbf{x}_{i,k+1}^{d}) + \sum_{j \in N_{i}} \mathbf{L}_{ij}(\mathbf{A}_{k}\mathbf{x}_{j,k} + \mathbf{B}_{k}\hat{\mathbf{u}}_{j,k} - \mathbf{x}_{j,k+1}^{d}) = \hat{\mathbf{A}}_{i,k}\mathbf{x}_{i,k} + \hat{\mathbf{B}}_{i,k}\hat{\mathbf{u}}_{i,k} - \hat{\mathbf{x}}_{i,k+1}^{d} + \sum_{i \in N_{i}} (\hat{\mathbf{A}}_{ij,k}\mathbf{x}_{j,k} + \hat{\mathbf{B}}_{ij,k}\hat{\mathbf{u}}_{j,k} - \hat{\mathbf{x}}_{ij,k+1}^{d})$$
(20)

where $\hat{A}_{i,k} = L_i A_k$, $\hat{A}_{ij,k} = L_{ij} A_k$, and similarly to other matrices. Further, define predict horizon of the solver as N_p and iterate the discrete dynamics (20) in the predict horizon $\begin{bmatrix} t_k, t_{k+N_p-1} \end{bmatrix}$. Define $E_{i,k} = \begin{bmatrix} e_{i,k+1}^T, e_{i,k+2}^T, \cdots, e_{k+N_p}^T \end{bmatrix}^T U_{i,k} = \begin{bmatrix} \hat{u}_{i,k}^T, \hat{u}_{i,k+1}^T, \cdots, \hat{u}_{k+N_p-1}^T \end{bmatrix}^T$ as sequences of error and control strategy, one has:

$$E_{i,k} = H_{i,k} x_{i,k} + W_{i,k} U_{i,k} - X_{i,k}^{d}$$

$$+ \sum_{j \in N_i} H_{j,k} x_{j,k} + W_{j,k} U_{j,k} - X_{j,k}^{d}$$

$$= H_{i,k} x_{i,k} + W_{i,k} U_{i,k} + S_{i,k}$$
(21)

where

$$\boldsymbol{H}_{i,k} = \begin{bmatrix} \hat{\boldsymbol{A}}_{i,k}^{\mathrm{T}} & \cdots & \left(\hat{\boldsymbol{A}}_{i,k}^{N_{p}}\right)^{\mathrm{T}} \end{bmatrix}^{\mathrm{T}}$$

$$\boldsymbol{W}_{i,k} = \begin{bmatrix} \hat{\boldsymbol{B}}_{i,k} & \cdots & 0 \\ \vdots & \ddots & \vdots \\ \hat{\boldsymbol{A}}_{i,k}^{N_{p}-1} \hat{\boldsymbol{B}}_{i,k} & \cdots & \hat{\boldsymbol{B}}_{i,k} \end{bmatrix}$$

$$\boldsymbol{X}_{i,k}^{d} = \begin{bmatrix} \hat{\boldsymbol{x}}_{i,k}^{\mathrm{T}} & \cdots & \hat{\boldsymbol{x}}_{i,k+N_{p}}^{\mathrm{T}} \end{bmatrix}^{\mathrm{T}}$$

$$\boldsymbol{S}_{i,k} = -\boldsymbol{X}_{i,k}^{d} + \sum_{j \in N_{i}} (\boldsymbol{H}_{j,k} \boldsymbol{x}_{j,k} + \boldsymbol{W}_{j,k} \boldsymbol{U}_{j,k} - \boldsymbol{X}_{j,k}^{d})$$

$$(22)$$

Secondly, do the same for the cost function, the discrete form and iterative form are:

$$J_{i} = \sum_{g=k}^{k+N_{p}-1} \left(\boldsymbol{e}_{i,g+1}^{\mathsf{T}} \boldsymbol{Q}_{i} \boldsymbol{e}_{i,g+1} + \hat{\boldsymbol{u}}_{i,g}^{\mathsf{T}} \boldsymbol{R}_{i} \hat{\boldsymbol{u}}_{i,g} + \sum_{j \in N_{i}} \hat{\boldsymbol{u}}_{j,g}^{\mathsf{T}} \boldsymbol{R}_{ij} \hat{\boldsymbol{u}}_{j,g} \right)$$

$$J_{i,k} = \boldsymbol{E}_{i,k}^{\mathsf{T}} \boldsymbol{Q}_{i,k} \boldsymbol{E}_{i,k} + \boldsymbol{U}_{i,k}^{\mathsf{T}} \boldsymbol{R}_{i,k} \boldsymbol{U}_{i,k} + \sum_{j \in N_{i}} \boldsymbol{U}_{j,k}^{\mathsf{T}} \boldsymbol{R}_{ij,k} \boldsymbol{U}_{j,k}$$

$$(23)$$

where $Q_{i,k} = I_{N_p} \otimes Q_i$, $R_{i,k} = I_{N_p} \otimes R_i$ and $R_{ij,k} = I_{N_p} \otimes R_{ij}$. However, the optimal control strategy of single MU cannot be solved independently due to the coupling in (22) and (23). In order to achieve distributed control, further decoupling of cost function is required. Substituting (22) into (23), one has:

$$J_{i,k} = \left(\boldsymbol{x}_{i,k}^{T} \boldsymbol{H}_{i,k}^{T} + \boldsymbol{S}_{i,k}^{T} \right) \boldsymbol{Q}_{i,k} \left(\boldsymbol{H}_{i,k} \boldsymbol{x}_{i,k} + \boldsymbol{S}_{i,k} \right)$$

$$+ \boldsymbol{U}_{i,k}^{T} \left(\boldsymbol{R}_{i,k} + \boldsymbol{W}_{i,k}^{T} \boldsymbol{Q}_{i,k} \boldsymbol{W}_{i,k} \right) \boldsymbol{U}_{i,k}$$

$$+ 2 \left(\boldsymbol{x}_{i,k}^{T} \boldsymbol{H}_{i,k}^{T} + \boldsymbol{S}_{i,k}^{T} \right) \boldsymbol{Q}_{i,k} \boldsymbol{W}_{i,k} \boldsymbol{U}_{i,k}$$

$$+ \sum_{i \in N_{i}} \boldsymbol{U}_{j,k}^{T} \boldsymbol{R}_{ij,k} \boldsymbol{U}_{j,k}$$

$$(24)$$

MU *i* can only optimize its individual control strategy, so terms in (24) without $U_{i,k}$ are omitted. Therefore, the cooperative game controller can be reformulated as the following quadratic programming (QP) problem:

$$\min_{U_{i,k}} J_{i,k} = \frac{1}{2} U_{i,k}^{\mathrm{T}} q_{i,k} U_{i,k} + p_{i,k}^{\mathrm{T}} U_{i,k}$$
 (25)

where

$$\mathbf{q}_{i,k} = 2\left(\mathbf{R}_{i,k} + \mathbf{W}_{i,k}^{T} \mathbf{Q}_{i,k} \mathbf{W}_{i,k}\right)$$

$$\mathbf{p}_{i,k} = 2\mathbf{W}_{i,k}^{T} \mathbf{Q}_{i,k} \left(\mathbf{H}_{i,k} \mathbf{x}_{i,k} + \mathbf{S}_{i,k}\right)$$
(26)

During the gaming process, MU i solve the above QP problem in each time t_k to achieve Pareto optimal, based on neighbor MU's control strategy sequences U_j and predicted state sequences X_j . After obtaining its own control strategy sequence U_i , the first term \hat{u}_i^* is extracted, and the actual control input is calculated as $u_i^* = \hat{u}_i^* - \hat{T}_i$.

Remark 3. Game model (15) includes the predicted tension force \hat{T}_i . By introducing it into dynamics, the effect of tension force on the game state e_i can be forecasted. Thus this effect can be reduced by active control. Unlike perturbation estimation methods, this approach does not require bounded assumptions about the perturbations themselves and their derivatives, which are generally unknown and highly conservative.

4. Simulation and results

In this section, numerical simulations are conducted to demonstrate the performance of the proposed cooperative game theory based formation controller. The simulation environment for TSNR is built based on MuJoCo [22], which is a high-fidelity open source physics engine considering complex dynamical effects and flexible constraints. The training data is collected from capture trajectories with random position of the target in MuJoCo. A total of 1000 trajectories are collected, each lasting 30 s for 30000 data points.

The orbit radius of space debris and TSNR is $r_0 = 42164$ km. The initial position of target is at $x_0 =$ $[5,0,0]^{T}$, and the initial states of four MUs when leaving the platform are $x_1(t_0) = [-10, 0.75, 0.75, 0, 0, 0]^T$, $[-10, -0.75, 0.75, 0, 0, 0]^{T}$ $x_2(t_0)$ $x_3(t_0)$ $[-10,0.75,-0.75,0,0,0]^{T}$ and $x_4(t_0)$ $[-10, -0.75, -0.75, 0, 0, 0]^{T}$, where the position and velocity units are m and m/s. Before capture, TSNR is stored in the platform and folded in a square pattern with mesh edge $l_m = 0.5 \,\mathrm{m}$. Then TSNR is released and the net is gradually expanded as large as possible before contact by the motion of four MUs. Two mission scenarios are considered: (1) Case 1: the target is stationary and TSNR moves directly to capture it. (2) Case 2: the target is rotating and TSNR moves to align with the target inertial spindle before capturing. To successfully capture the target, the net should close completely after contact and envelope it, so the terminal condition of four MUs are $\mathbf{x}_1(t_f) = [5, 0.5, 0.5, 0, 0, 0]^T$, $\mathbf{x}_2(t_f) =$ $[5, -0.5, 0.5, 0, 0, 0]^{T}$, $x_3(t_f) = [5, 0.5, -0.5, 0, 0, 0]^{T}$ and $x_4(t_f) = [5, -0.5, -0.5, 0, 0, 0]^{T}$ in Case 1, $[3.41, 5.43, 0.50, 0.25, 0.43, 0]^{T}$ $\boldsymbol{x}_1(t_f)$ $[3.91, 4.56, 0.50, 0.25, 0.43, 0]^{T}$ $\mathbf{x}_2(t_f)$ = $[3, 91, 4.56, -0.50, 0.25, 0.43, 0]^{T}$ and $x_4(t_f) = [3.41, 5.43, -0.50, 0.25, 0.43, 0]^T$ in Case 2 respectively. The other detailed parameters of TSNR is shown in [4].

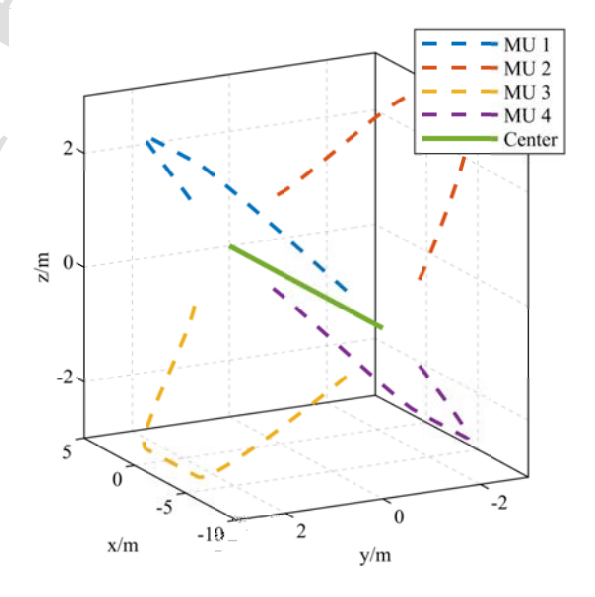


Fig. 4. Three-dimensional diagram of planned trajectories of four MUs and their center in Case 1.

The capture trajectories for the two cases planned by method [8] are depicted in Fig. 4 and Fig. 5. According

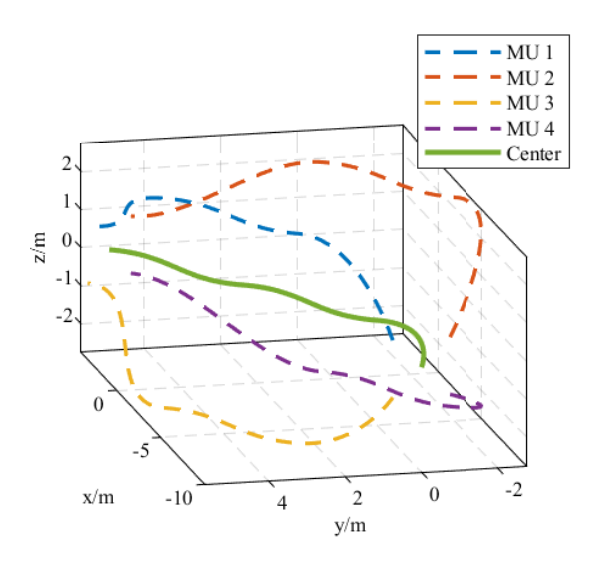


Fig. 5. Three-dimensional diagram of planned trajectories of four MUs and their center in Case 2.

to the mission description, four MUs in each case need to open the net, then drive it moving forward, and finally envelop the target. Case 2 has a more complex trajectory compared to Case 1, as MUs need to manoeuvre to adjust the configuration of the net for the rotating target.

The envelope capture sequence of TSNR in Case 1 is illustrated in Fig. 6, depicting the action of the designed cooperative formation controller. Upon release from the platform satellite, four MUs progressively move away to expand the net. As the net reaches its maximum size, MUs drive it closer to space debris (depicted as the green cylinder in Fig. 6). It's evident that in the final moments, the net can completely encircle the target, thereby completing the debris capture mission. Fig. 7 shows the capture process of TSNR in Case 2, where the target rotation adds considerable difficulty to the capture task. After fully deploying the flexible net (at 10 s), four MUs continuously move the position of the flexible net and adjust the angle of the flexible net to align with the inertial spindle of the target (10 - 20 s), while maintaining the size of the flying net and approaching the target. At 30 s, the debris is finally captured by TSNR.

Fig. 8 and Fig. 9 depict tension forces acting on each MU obtained by the proposed neural network estimator in each case. It is clear that during the approaching phase (0 - 10 s), the tension force acting on each MU is quite small or even negligible. This phenomenon is due to the net not being taut enough to generate significant force. But the manoeuvre of MUs in this phase

will create extra tension forces on each other at a later time. When the net is fully deployed $(10-20\,\mathrm{s})$, tension force increases substantially, enabling each MU to interact with others through this force transmission. After the net makes contact with debris (at 20 s), the net is no longer taut and the tension force again becomes a very small value. During the envelope phase, a collision force is generated. However, the impact of the collision is not discussed in this paper for simplicity. The higher forces in Case 2 compared to that in Case 1 are due to the more complex trajectory of TSNR when catching a spinning target. The four MUs have to perform turning manoeuvres as well as adjusting the position and attitude of the net.

To demonstrate the effectiveness of the proposed method (AEMC), it is compared with two kinds of force-compensation methods, a Distributed Model Predict Control (DMPC) scheme and a Sliding Mode Control (SMC) approach [23]. Taking MU 1 as an example, the position tracking error curves of three directions under these three algorithms in Case 1 are illustrated in Fig. 10. It's evident that the X-direction error under the proposed method converges the fastest (as shown in Fig. 10 (a)). The other two methods both have a peak at 10 s, the moment when the net is fully deployed and there is a sudden change in tension force (as shown in Fig. 8). Force-compensation methods only compensate for perturbations when they occur, while the proposed energy management approach can effectively predict, estimate, and utilize the tension forces in advance.

In the Y and Z directions (as illustrated in Fig. 10 (b) and (c)), there is also a peak at 10 s for both forcecompensation methods, whereas the proposed method has converged by this time. It's worth noting that all three algorithms produce large errors in the Y and Z directions during the approach phase (0-10 s) and enclosing phase (20-30 s). The proposed energy management approach not only has a smaller error but also produces in a different direction than the other two methods. This is the difference between energy management and force compensation. Based on the predicted forces and interactions, MUs communicate and gamble collaboratively to reach the Pareto Optimal Solution. The game state of the MUs consists of two parts, one of which is explicitly embodied in the cost function (16) in the form of cooperative consensus error (14), and the other is implicitly embodied in the optimization variables \hat{u}_i in the form of tension force T_i acting by other satellites, guaranteeing that each MU's strategy is the best response relative to the strategies of its collaborators.

Fig. 11 compares the performance of the three controllers in Case 2. It can be seen that AEMC performs

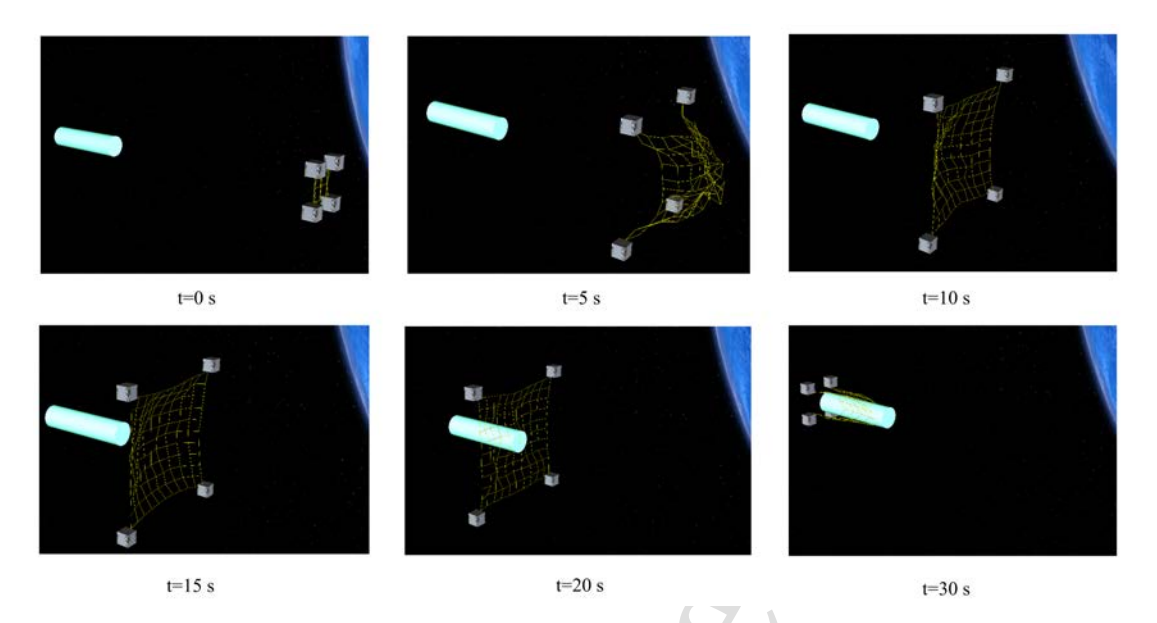


Fig. 6. Envelope capture sequence of TSNR in Case 1.

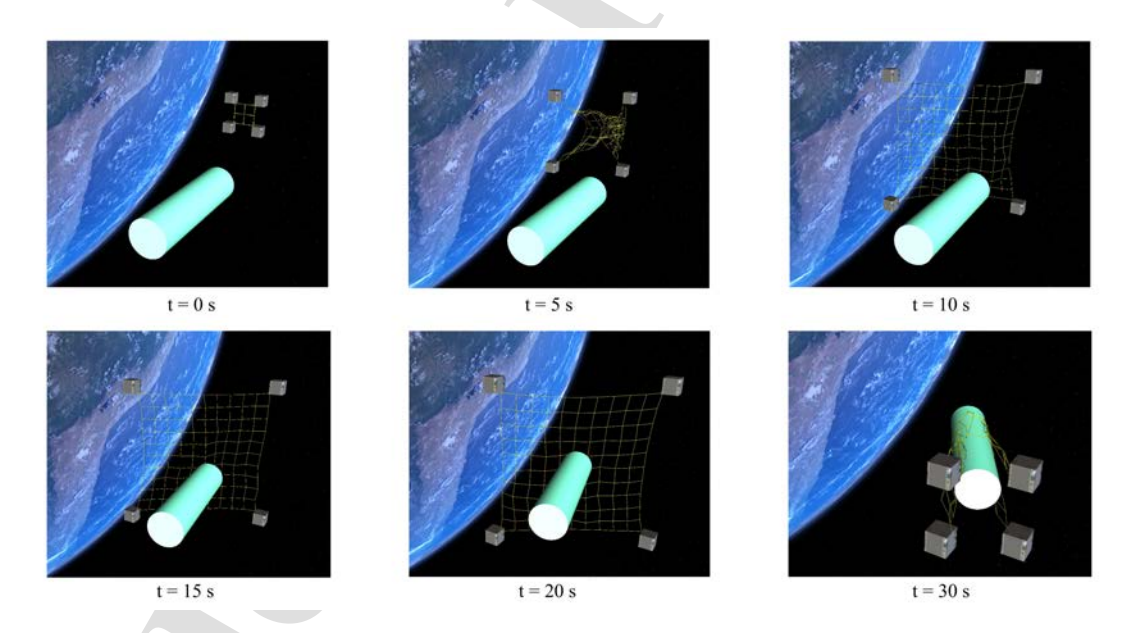


Fig. 7. Envelope capture sequence of TSNR in Case 2.

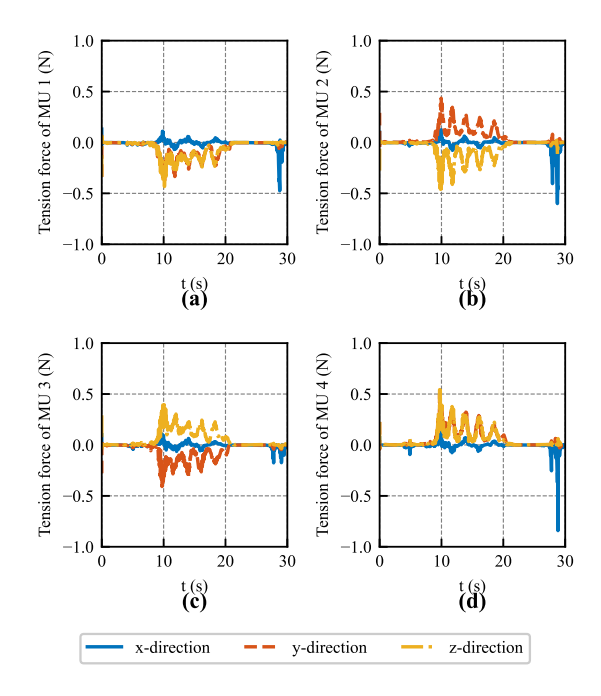


Fig. 8. Predicted tension forces of four MUs in Case 1. (a) MU 1. (b) MU 2. (c) MU 3. (d) MU 4.

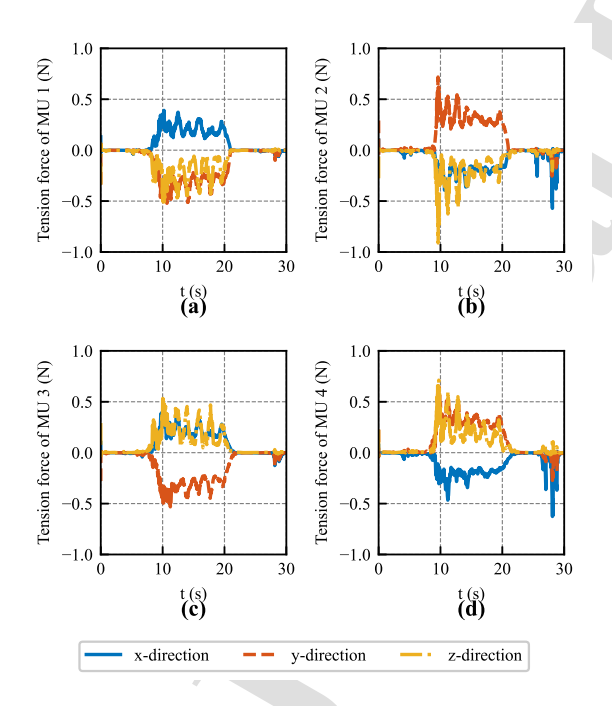


Fig. 9. Predicted tension forces of four MUs in Case 2. (a) MU 1. (b) MU 2. (c) MU 3. (d) MU 4.

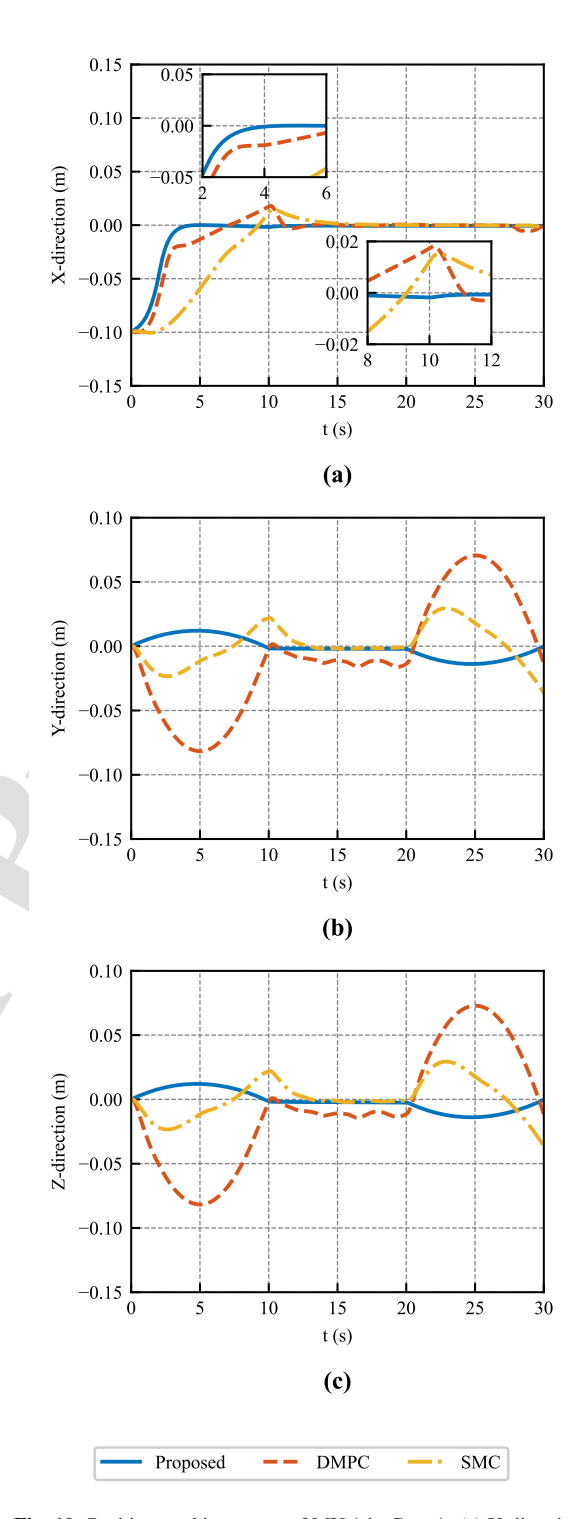


Fig. 10. Position tracking errors of MU 1 in Case 1. (a) X-direction. (b) Y-direction. (c) Z-direction.

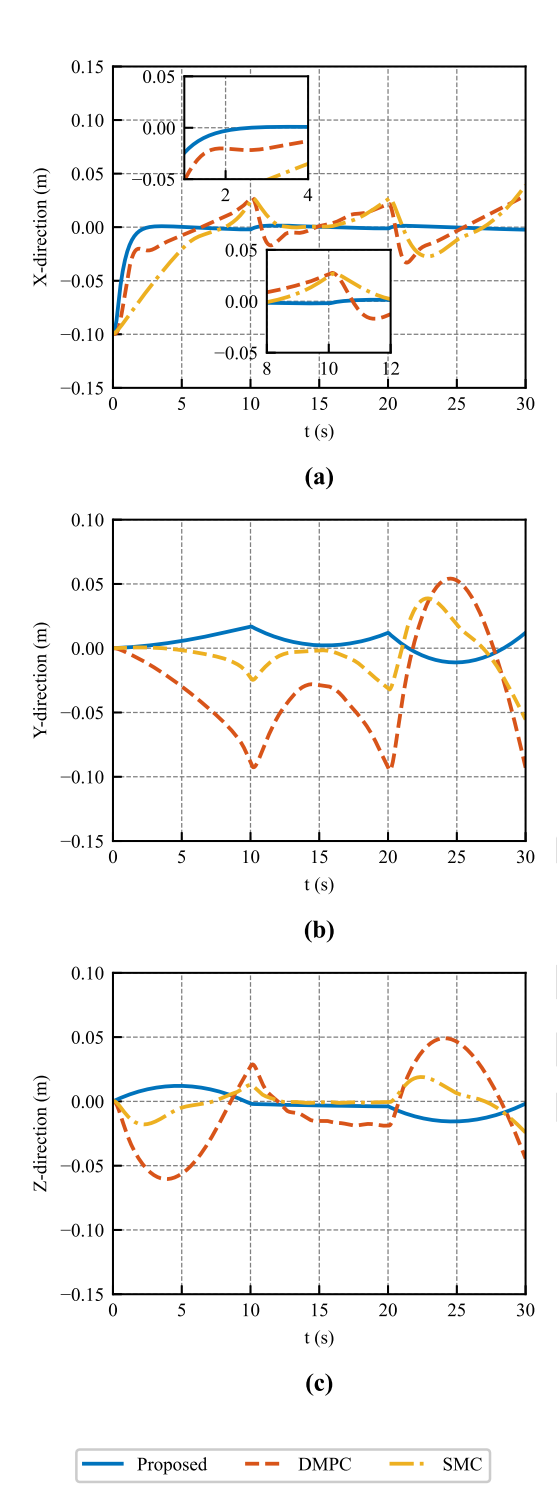


Fig. 11. Position tracking errors of MU 1 in Case 2. (a) X-direction. (b) Y-direction. (c) Z-direction.

much better than the other two algorithms when faced with complex trajectories. In the flexible net position and attitude adjustment phase (10 - 20 s), both two compensation-based methods show large tracking errors compared to Fig. 10. In contrast, the AEMC proposed in this paper is still able to limit the error to a quite narrow range.

Table. 1. Fuel consumption of TSNR in Case 1.

MU	AEMC (N)	DMPC (N)	SMC (N)
1	35.19	35.44	37.08
2	35.23	35.23	37.21
3	35.13	34.87	37.12
4	35.22	35.44	37.27
Total	140.77	140.98	148.68

Table. 2. Fuel consumption of TSNR in Case 2.

MU	AEMC (N)	DMPC (N)	SMC (N)
1	56.21	55.32	55.78
2	55.16	56.50	56.56
3	56.21	55.23	55.79
4	55.18	55.32	56.56
Total	222.77	223.53	224.71

The fuel consumption caused by each algorithm in the two space debris capture tasks are given in Table.1 and Table.2, expressed in terms of the total control input generated. It can be seen that the SMC method consumes the most and the proposed method consumes the least, effectively demonstrating the validity of the energy management approach. And the consumption of the DMPC method and the proposed method are very close to each other, which may be because both algorithms use the concept of prediction-optimization. However, in conjunction with Fig. 10 and Fig. 11, compared to DMPC, the proposed AEMC method performs better at almost the same fuel consumption. A portion of the fuel consumption of the DMPC algorithm is used for tension force compensation, while the proposed AEMC approach uses this consumption to improve control performance.

5. Conclusion

This paper proposes a novel strategy to tackle the challenges associated with capturing space debris and

tracking a specific trajectory for TSNR. The proposed strategy combines principles from both differential game and machine learning theory, aimed at efficiently completing the capture mission. The conclusions are outlined as follows:

- A novel active energy management framework (AEMC) is established to conserve fuel consumption, by actively managing tension forces on the net and maximizing their benefit to control effectiveness.
- A DNN based force estimator is developed to depict the intricate time-delayed interactions among MUs, facilitating the precise estimation and prediction of tension force. And a predictive dynamic model is introduced according to it.
- Using cooperative game theory, a formation tracking control strategy is proposed to deeply reflect the relationship among MUs. Each MU optimise its cost function in a fully distributed manner to suppress the tracking error and achieve consensus.
- 4. Numerical simulations demonstrate the effectiveness of the proposed strategy in the mission of capturing space debris utilizing TSNR.

Appendix: Detailed Proof of Theorem 1

Lemma 1. [24] For any $|x| \le M$ and $|y| \le M$, M is positive, there is a ReLU network with two input satisfies: $|\eta(x, y) - xy| \le \sigma$, $\sigma \in (0, 1)$.

Proof: Define N as a positive integer, $\mathbf{x} \in [0, 1]^d$ and $\mathbf{m} = (m_1, m_2, \dots m_d) \in \{0, 1, \dots, N\}^d$, function f can be expanded to a n-1 order Taylor polynomial at $\mathbf{x} = \frac{m}{N}$:

$$P_m(x) = \sum_{m \mid n| < n} a_{m,n} \left(x - \frac{m}{N} \right)^n \tag{27}$$

where $a_{m,n} = \frac{d^n f}{n!}|_{x=\frac{m}{N}}$, and $|a_{m,n}| \leq 1$, $\left(x-\frac{m}{N}\right)^n = \prod_{k=1}^d (x_k - \frac{m_k}{N})$. Then, approximate f by a sum-product combination f_1 :

$$f_1 = \sum_{m \in \{0,1,\dots,N\}^d} Q_m(x) P_m(x)$$
 (28)

where $Q_m(x) = \prod_{k=1}^d q\left(3N\left(x_k - \frac{m_k}{N}\right)\right)$ and $\sum Q_m(x) \equiv 1$. q(x) has the following form:

$$q(x) = \begin{cases} 1, & |x| < 1, \\ 0, & 2 < |x|, \\ 2 - |x|, & 1 \le |x| \le 2 \end{cases}$$
 (29)

With the property of functions, $|q(x)|_{\infty} = |Q_m(x)|_{\infty} = 1$, and supp $Q_m(x) \subset \left\{x : \left|x_k - \frac{m_k}{N}\right| < \frac{1}{N}\right\}$, the error between f_1 and f can be calculated as:

$$|f - f_{1}|_{\infty} = \left| \sum_{m} Q_{m}(x) \left(f(x) - P_{m}(x) \right) \right|$$

$$\leq \sum_{m: |x_{k} - \frac{m_{k}}{N}| < \frac{1}{N}} |f(x) - P_{m}(x)|$$

$$\leq 2^{d} \max_{m: |x_{k} - \frac{m_{k}}{N}| < \frac{1}{N}} |f(x) - P_{m}(x)| \qquad (30)$$

$$\leq \frac{2^{d} d^{n}}{n!} \left(\frac{1}{N} \right)^{n} \max_{n: |n| = n} \operatorname{ess}_{x \in [0, 1]^{d}} |d^{n} f(x)|$$

$$\leq \frac{2^{d} d^{n}}{n!} \left(\frac{1}{N} \right)^{n}$$

Next, design a ReLU neural network f_2 to approximate f_1 . Combine (27) and (28), f_1 can be expanded as $\sum_{m \in \{0,...,N\}^d} \sum_{n:|n| < n} a_{m,n} Q_m(x) \left(x - \frac{m}{N}\right)^n$. Correspondingly, f_2 is given as:

$$f_2 = \sum_{m \in \{0, \dots, N\}^d} \sum_{n : |n| < n} a_{m,n} K(x)$$
 (31)

Based on Lemma1, K(x) is the approximation of the product $Q_m(x)\left(x-\frac{m}{N}\right)^n$ in f_1 . It can be obtained by the application of η :

$$K(\mathbf{x}) = \eta(q(3Nx_1 - m_1), \eta(q(3Nx_2 - m_2), \dots, \eta(x_1 - \frac{m_1}{N}, \eta(x_2 - \frac{m_2}{N}, \dots))))$$
(32)

Note that $|q(3Nx_k - m_k)| \le 1$ and $|x_k - \frac{m_k}{N}| \le 1$. Repeatedly applying Lemma 1, every multiplication in (32) is bounded by M = d + n, while there are d factors of $q(3Nx_k - m_k)$ and at most n - 1 factors of $x_k - \frac{m_k}{N}$ in term $Q_m(x)\left(x - \frac{m}{N}\right)^n$. Then the error between f_2 and f_1 is calculated as:

$$|f_{2} - f_{1}|_{\infty}$$

$$= \left| \sum_{m \in \{0, \dots, N\}^{d}} \sum_{n: |n| < n} a_{m,n} \left(K(x) - Q_{m}(x) \left(x - \frac{m}{N} \right)^{n} \right) \right|$$

$$= \left| \sum_{m: x \in \text{supp } Q_{m}} \sum_{n: |n| < n} a_{m,n} \left(K(x) - Q_{m}(x) \left(x - \frac{m}{N} \right)^{n} \right) \right|$$

$$\leq 2^{d} \max_{m: x \in \text{supp } Q_{m}} \sum_{n: |n| < n} \left| K(x) - Q_{m}(x) \left(x - \frac{m}{N} \right)^{n} \right|$$

$$\leq 2^{d} d^{n} (d+n) \sigma$$

$$(33)$$

Finally, defining $N = \left[\left(\frac{n!}{2^d d^n} \frac{\epsilon}{2} \right)^{-1/n} \right]$ and $\sigma = \frac{\epsilon}{2^{d+1} d^n (d+n)}$, (30) and (33) leads to the conclusion:

$$|f_2 - f|_{\infty} \leqslant |f_2 - f_1|_{\infty} + |f_1 - f|_{\infty}$$

$$\leqslant \frac{\epsilon}{2} + \frac{\epsilon}{2} = \epsilon$$
(34)

Declaration of competing interest

The authors state that they have no known competing financial or personal interests that could influence the work reported in this publication.

Acknowledgements

This research was funded by the National Natural Science Foundation of China under Grant Nos.62222313, 62173275, 62327809, 62303381, and 62303312.

References

- E. G. Asri, Z. H. Zhu, An introductory review of swarm technology for spacecraft on-orbit servicing, Int. Journal of Mech. Sys. Dyn. 4 (1) (2024) 3–21. doi:10.1002/msd2.12098.
- [2] R. Benvenuto, S. Salvi, M. Lavagna, Dynamics analysis and GNC design of flexible systems for space debris active removal, Acta. Astronaut. 110 (2015) 247–265. doi:10.1016/ j.actaastro.2015.01.014.
- [3] Y. Zhang, P. Huang, Z. Meng, Z. Liu, Precise angles-only navigation for noncooperative proximity operation with application to tethered space robot, IEEE Trans. Contr. Syst. Technol. 27 (3) (2019) 1139–1150. doi:10.1109/TCST.2018.2790400.
- [4] F. Zhang, P. Huang, Releasing dynamics and stability control of maneuverable tethered space net, IEEE/ASME Trans. Mechatron. 22 (2) (2017) 983–993. doi:10.1109/TMECH.2016. 2628052.
- [5] H. Wen, Z. H. Zhu, D. Jin, H. Hu, Constrained tension control of a tethered space-tug system with only length measurement, Acta. Astronaut. 119 (2016) 110–117. doi:10.1016/j.actaastro.2015.11.011.
- [6] Y. Liu, F. Zhang, P. Huang, Coordinated control for constrained multiple spacecraft system, IEEE Trans. Aerosp. Electron. Syst. 56 (2) (2020) 1189–1201. doi:10.1109/TAES. 2019.2926612.
- [7] F. Zhang, P. Huang, Fuzzy-based adaptive super-twisting sliding-mode control for a maneuverable tethered space net robot, IEEE Trans. Fuzzy Syst. 29 (7) (2021) 1739–1749. doi: 10.1109/TFUZZ.2020.2985325.
- [8] Y. Liu, Z. Ma, F. Zhang, P. Huang, Time-Varying Formation Planning and Scaling Control for Tethered Space Net Robot, IEEE Trans. Aerosp. Electron. Syst. 59 (5) (2023) 6717–6728. doi:10.1109/TAES.2023.3276742.
- [9] L. Jiang, F. Gonzalez, A. McFadyen, Cooperative Game Theory based Multi-UAV Consensus-based Formation Control, in: 2020 International Conference on Unmanned Aircraft Systems (ICUAS), IEEE, Athens, Greece, 2020, pp. 93–99. doi:10. 1109/ICUAS48674.2020.9213841.

- [10] J. Li, S. Chen, C. Li, F. Wang, Distributed Game Strategy for Formation Flying of Multiple Spacecraft With Disturbance Rejection, IEEE Trans. Aerosp. Electron. Syst. 57 (1) (2021) 119– 128. doi:10.1109/TAES.2020.3010593.
- [11] N. Han, J. Luo, L. Zong, Cooperative Game Method for On-Orbit Substructure Transportation Using Modular Robots, IEEE Trans. Aerosp. Electron. Syst. 58 (2) (2022) 1161–1175. doi: 10.1109/TAES.2021.3111141.
- [12] Y. Liu, Z. Ma, F. Zhang, P. Huang, Y. Lu, H. Chang, Coordinated transportation of tethered multi-rotor UAVs based on differential graphical games, Aerosp. Sci. Technol. 148 (2024) 109078. doi:10.1016/j.ast.2024.109078.
- [13] Y. Liu, F. Zhang, P. Huang, Y. Lu, Fixed-time consensus tracking for second-order multiagent systems under disturbance, IEEE Trans. Syst. Man Cybern, Syst. 51 (8) (2021) 4883–4894. doi:10.1109/TSMC.2019.2944392.
- [14] B. Ning, J. Jin, J. Zheng, Z. Man, Finite-time and fixed-time leader-following consensus for multi-agent systems with discontinuous inherent dynamics, Int J Control 91 (6) (2018) 1259– 1270. doi:10.1080/00207179.2017.1313453.
- [15] S. Li, C. Liu, Z. Sun, Finite-time distributed hierarchical control for satellite cluster with collision avoidance, Aerosp. Sci. Technol. 114 (2021) 106750. doi:10.1016/j.ast.2021.106750.
- [16] Y. Hua, X. Dong, L. Han, Q. Li, Z. Ren, Finite-time time-varying formation tracking for high-order multiagent systems with mismatched disturbances, IEEE Trans. Syst. Man Cybern, Syst. (2019) 1–9doi:10.1109/TSMC.2018.2867548.
- [17] A. Jin, F. Zhang, P. Huang, Learning-based data-driven optimal deployment control of tethered space robot, Adv. Space Res. 74 (5) (2024) 2214–2224. doi:https://doi.org/10.1016/ i.asr.2024.04.032.
- [18] G. Shi, X. Shi, M. O'Connell, R. Yu, K. Azizzadenesheli, A. Anandkumar, Y. Yue, S.-J. Chung, Neural Lander: Stable Drone Landing Control Using Learned Dynamics, in: 2019 International Conference on Robotics and Automation (ICRA), IEEE, Montreal, QC, Canada, 2019, pp. 9784–9790. doi: 10.1109/ICRA.2019.8794351.
- [19] G. Torrente, E. Kaufmann, P. Fohn, D. Scaramuzza, Data-Driven MPC for Quadrotors, IEEE Robot. Autom. Lett. 6 (2) (2021) 3769–3776. doi:10.1109/LRA.2021.3061307.
- [20] M. O'Connell, G. Shi, X. Shi, K. Azizzadenesheli, A. Anandkumar, Y. Yue, S.-J. Chung, Neural-Fly enables rapid learning for agile flight in strong winds, Sci. Robot. 7 (66) (2022) eabm6597. doi:10.1126/scirobotics.abm6597.
- [21] M. Farina, P. Amato, On the optimal solution definition for many-criteria optimization problems, in: 2002 Annual Meeting of the North American Fuzzy Information Processing Society Proceedings. NAFIPS-FLINT 2002 (Cat. No. 02TH8622), IEEE, New Orleans, LA, USA, 2002, pp. 233–238. doi: 10.1109/NAFIPS.2002.1018061.
- [22] E. Todorov, T. Erez, Y. Tassa, MuJoCo: A physics engine for model-based control, in: 2012 IEEE/RSJ International Conference on Intelligent Robots and Systems, IEEE, Vilamoura-Algarve, Portugal, 2012, pp. 5026–5033. doi:10.1109/IROS. 2012.6386109.
- [23] Y. Ma, Y. Zhang, P. Huang, Y. Liu, F. Zhang, Game theory based finite-time formation control using artificial potentials for tethered space net robot, Chin. J. Aeronaut. 37 (8) (2024) 358–372. doi:https://doi.org/10.1016/j.cja.2024.04.011.
- [24] D. Yarotsky, Error bounds for approximations with deep ReLU networks, Neural Networks 94 (2017) 103–114. doi:10. 1016/j.neunet.2017.07.002.

Highlights

- A novel approach for the application of Tethered Space Net Robot (TSNR) in space debris removal is investigated.
- An active energy management framework is established to mitigate the negative effects and capitalize on the positive effects of tension force.
- A Deep Neural Network (DNN) based estimator is proposed to estimate and predict tension force among Maneuverable Units (MUs).
- A distributed cooperative game theory based control scheme is designed. An MU can actively manage the effects of others.

Declaration of interests
☑ The authors declare that they have no known competing financial interests or personal relationships that could have appeared to influence the work reported in this paper.
☐ The author is an Editorial Board Member/Editor-in-Chief/Associate Editor/Guest Editor for [Journal name] and was not involved in the editorial review or the decision to publish this article.
☐ The authors declare the following financial interests/personal relationships which may be considered as potential competing interests: